Cell-Free MIMO-Assisted ISAC: Joint AP Switching and Power Allocation

Bin Yan[1], Zheng Wang[1], Amin Sakzad[2], Yongming Huang[1], and Michail Matthaiou[3]
[1]School of Information Science and Engineering, Southeast University, Nanjing, China
[2]Department of Software Systems & Cybersecurity, Monash University, Melbourne, Australia
[3]Centre for Wireless Innovation (CWI), Queen's University, Belfast, U.K.
E-mail: bin_yan@seu.edu.cn; wznuaa@gmail.com; Amin.Sakzad@monash.edu; huangym@seu.edu.cn; m.matthaiou@qub.ac.uk

***Abstract*—This paper investigates a distributed implementation of integrated sensing and communication (ISAC) based on cell-free massive MIMO (CF-mMIMO). To satisfy the multi-target sensing requirements and achieve maximum user fairness, the access points (APs) can be dynamically switched between communication and sensing modes, with their transmit power adaptively adjusted according to the service demands. This operational flexibility, however, leads to a complex mixed-integer non-convex optimization problem. To circumvent the high computational complexity associated with traditional solutions, we reformulate the original problem by leveraging the coupling relationship between the coefficients of AP mode switching and power allocation, thus approximating it as a non-convex optimization within the continuous domain. The resulting problem is then efficiently solved using the penalty and accelerated proximal gradient with adaptive momentum (APG-AM) method, which we label as smooth characterization joint AP switching and power allocation (SC-JAPSPA) algorithm. Simulation results demonstrate that the proposed algorithm achieves up to 95% of the performance delivered by state-of-the-art benchmarks, while reducing the computational time by more than an order of magnitude.**

***Index Terms*—Accelerated proximal gradient, CF-mMIMO, ISAC, mixed-integer non-convex optimization.**

I. Introduction

As a cornerstone of future wireless networks, integrated sensing and communication (ISAC) enables the joint exploitation of the radio spectrum for dual purposes, paving the way for the efficient co-existence of sensing and communication under limited resources [1]. However, in realistic scenarios, the simultaneous operation of multiple ISAC base stations over the same area, frequency band, and time will lead to inevitable interference. Such a setup will naturally compromise the performance of both sensing and communication. This motivates the recent and widespread interest in distributed CF-mMIMO-assisted ISAC systems [1]–[6].

In such systems, effective resource allocation plays a critical role in facilitating both communication and sensing. Specifically, [2] considered designing power allocation schemes to enhance the system performance metrics. However, they rely on static access point (AP) operating modes in which each AP simultaneously participates in sensing and communication tasks, leading to unavoidable signal interference and an increased risk of information leakage [7]. In contrast to the static AP operation, the work in [1] advanced the field by proposing a dynamic AP mode switching strategy, which partitions the APs into two disjoint communication APs (C-AP) and sensing APs (S-AP) sets, thereby enabling more effective interference management. More specifically, the introduction of AP mode switching brings complex discrete characteristics into the optimization problem in hand. To address this, [1] adopted a successive convex approximation (SCA) framework to obtain a feasible solution. However, this approach requires computing second-order Hessian matrices, which becomes prohibitively expensive in terms of both computation and memory as the communication dimensions and sensing coverage increase [8].

Corresponding author: Zheng Wang (e-mail: wznuaa@gmail.com).

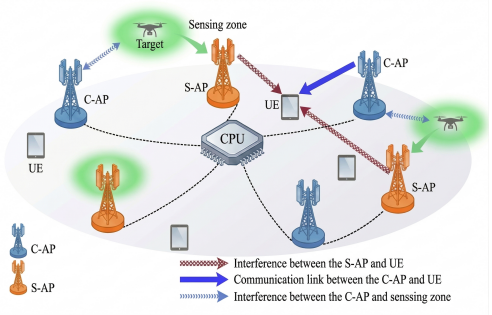

Fig. 1. Illustration of the considered CF-mMIMO-assisted ISAC system.

To solve the above joint AP switching and power allocation (JAPSPA) problem more efficiently, this paper revisits the coupling relationship between discrete and continuous optimization variables. A smooth characterization method is proposed, where continuous variables are used to approximate the step-function behavior of discrete variables, thereby transforming the original problem into a continuous one. Furthermore, a nested solution framework is developed by combining the penalty method with the APG-AM method, resulting in the smooth characterization (SC)-JAPSPA algorithm that efficiently solves the transformed non-convex problem. Simulation results demonstrate that the proposed algorithm achieves almost comparable performance to the benchmark methods with significantly reduced computational complexity.

II. System Model

Consider a canonical CF-mMIMO downlink system operating under time division duplex (TDD). In this system, M

multi-antenna APs, equipped with uniform linear arrays of N antennas, serve K single-antenna users and simultaneously radiate probing signals toward L designated sensing zones. For simplicity, we define the sets $\mathcal{M} \triangleq \{1,\ldots,M\}$, $\mathcal{K} \triangleq \{1,\ldots,K\}$ and $\mathcal{L} \triangleq \{1,\ldots,L\}$ to represent the indices of APs, users, and sensing zones, respectively. Following prior work [1], we assume a quasi-static channel model where each coherence interval spans a duration of τ symbols. The entire duration is divided into two parts: τ_u is allocated for uplink channel estimation and the remaining duration $\tau_d \triangleq \tau - \tau_u$ is for downlink information transfer and target detection.

A. Channel Model and Uplink Training

For the sensing channel model, we assume there is a line-of-sight (LoS) path between the sensing area and each AP, which is a commonly adopted model in literature [1], [2]. Then, the LoS channel $\overline{\mathbf{g}}_{ml} \in \mathbb{C}^N$ between the m-th AP and l-th sensing area is given by

$$\overline{\mathbf{g}}_{ml} = \sqrt{\zeta_{ml}}\mathbf{a}_N(\theta_{ml}),\ \forall m \in \mathcal{M}, \forall l \in \mathcal{L}, \tag{1}$$

where ζ_{ml} denotes the path loss. Moreover, $\mathbf{a}_N(\theta_{ml}) \in \mathbb{C}^N$ is the antenna array response vector from the m-th AP towards the l-th sensing area, and its n-th entry is modeled as

$$[\mathbf{a}_N(\theta_{ml})]_n = \exp\left(j\frac{2\pi d}{\lambda}(n-1)\sin(\theta_{ml})\right). \tag{2}$$

Here, d and λ denote the AP antenna spacing and carrier wavelength, respectively; θ_{ml} represents the angle of departure (AoD) associated with the m-th AP towards the l-th sensing area. Specifically, the propagation channel between the m-th AP and the k-th user is modeled as $\mathbf{g}_{mk} = \sqrt{\beta_{mk}}\mathbf{h}_{mk}$, with β_{mk} denoting the large-scale fading coefficient (LSFC), and $\mathbf{h}_{mk}$ is a small-scale fading vector with independent and identically distributed (i.i.d.) elements as $\mathcal{CN}(0,1)$. Assuming sufficient pilot resources, uplink training estimates the channel state information (CSI). The resulting minimum mean-square error (MMSE) estimate $\widehat{\mathbf{g}}_{mk}$ follows $\mathcal{CN}(\mathbf{0}_N, \gamma_{mk}\mathbf{I}_N)$, with mean-square value $\gamma_{mk} \triangleq \frac{\rho_u\tau_u\beta_{mk}^2}{1+\rho_u\tau_u\beta_{mk}}$, where ρ_u is the normalized transmit power of each pilot symbol.

B. Data and Probing Signal Transmission

To efficiently manage beamforming and power allocation while mitigating information leakage, a network-assisted full-duplex CF-mMIMO architecture was proposed in [7]. In this architecture, APs are dynamically assigned to a single operational mode based on system demands. For ISAC scenarios, the APs are divided into two disjoint subsets, the C-AP and S-AP subsets [1], represented by the following binary indicator

$$a_m = \begin{cases} 1, & \text{if } m\text{-th AP operates as C-AP,} \\ 0, & \text{if } m\text{-th AP operates as S-AP.} \end{cases} \tag{3}$$

As for C-APs, a fully distributed partial zero-forcing (PZF) precoding scheme is adopted to mitigate interference under the distributed implementation [9]. For a fixed m-th AP, users are categorized into disjoint strong and weak user groups (i.e., $\mathcal{S}_m$ and $\mathcal{W}_m$, $\mathcal{S}_m \cap \mathcal{W}_m = \oslash, |\mathcal{S}_m| + |\mathcal{W}_m| = K$), which are served by full-pilot ZF (FZF) precoding and maximum ratio transmission (MRT) precoding, respectively. Consistent with [9], the UE grouping can be based on the following rule

$$\sum_{k=1}^{|\mathcal{S}_m|} \frac{\overline{\beta}_{mk}}{\sum_{t\in\mathcal{K}}\beta_{mt}} \geq \varrho\%, \quad \forall m \in \mathcal{M}, \tag{4}$$

where $\{\overline{\beta}_{m1},\ldots,\overline{\beta}_{mK}\}$ indicates the set of LSFC sorted in descending order. The above criterion means that the m-th AP continuously selects users with higher channel gains to join the strong user group until their combined channel gain reaches $\varrho\%$ of the total. Thus, the transmit signal form the m-th C-AP can be expressed as

$$\mathbf{x}_m^c = \sum_{k\in\mathcal{S}_m}\sqrt{\rho_d\eta_{mk}^c}\mathbf{t}_{mk}^F x_k^c + \sum_{k\in\mathcal{W}_m}\sqrt{\rho_d\eta_{mk}^c}\mathbf{t}_{mk}^M x_k^c. \tag{5}$$

Here, ρ_d represents the normalized downlink transmit power, η_{mk}^c is the power allocation coefficient (PAC) of the m-th C-AP for the k-th user, while x_k^c is the symbol intended for the k-th user. Moreover, $\mathbf{t}_{mk}^F \in \mathbb{C}^N$ and $\mathbf{t}_{mk}^F \in \mathbb{C}^N$ represent the FZF and MRT precoding vectors, respectively [9].

On the other hand, S-AP m will transmit integrated probing signals for the purpose of detecting all regions. Specifically, the baseband signal at direction θ_{ml} can be written as [1]

$$\mathbf{x}_m^s = \sum_{l\in\mathcal{L}}\sqrt{\rho_d\eta_{ml}^s}\mathbf{a}_N(\theta_{ml})x_{ml}^s, \tag{6}$$

where η_{ml}^s is the non-negative PAC of S-AP m related to the sensing area l, while x_{ml}^s is the radar sensing symbol from S-AP m for sensing the area l.

In summary, the signal vector transmitted from AP m can be expressed as

$$\mathbf{x}_m = a_m\mathbf{x}_m^c + (1-a_m)\mathbf{x}_m^s. \tag{7}$$

C. Downlink SE and MASR

In the scenario where C-APs and S-APs transmit signals simultaneously, the signals from other users' encoding and the dedicated sensing signals are both treated as equivalent noise from the perspective of a typical k-th user. Based on the *use-and then-forget principle* [1], the signal-to-interference-plus-noise ratio (SINR) of user k is given in (8) on next page, while the values of ϱ_{mk} and ϖ_{mk} are determined by the precoding scheme of the AP for its associated users, such that

$$(\varrho_{mk}, \varpi_{mk}) = \begin{cases} (1, \frac{\beta_{mk}-\gamma_{mk}}{N-|\mathcal{S}_m|}), & \text{if user } k \in \mathcal{S}_m, \\ (N, N\beta_{mk}), & \text{if user } k \in \mathcal{W}_m. \end{cases} \tag{9}$$

Then, the achievable downlink spectral efficiency (SE) of the k-th user can be obtained by *Shannon's theorem*, i.e.,

$$\mathrm{SE}_k(\mathbf{\Theta}^c, \mathbf{\Theta}^s) = \left(1-\frac{\tau_u}{\tau}\right)\log_2\left(1+\mathrm{SINR}_k\left(\mathbf{\Theta}^c, \mathbf{\Theta}^s\right)\right), \tag{10}$$

where $\mathbf{\Theta}^c \in \mathbb{R}_+^{M\times K}$ and $\mathbf{\Theta}^s \in \mathbb{R}_+^{M\times L}$ are the matrices of communication and sensing PACs, with their (m,k)-th and (m,l)-th entries denoted by η_{mk}^c and η_{ml}^s, respectively. For the subsequent optimization of sensing performance, we adopt the

mainlobe-to-average-sidelobe ratio (MASR) metric as defined in (11), following the work of [1]. Analogously, the value of ν_{mk} is linked to the user's assigned precoding subset. For a given m-th AP, the parameter $\nu_{mk} = \frac{1}{N-|\mathcal{S}_m|}$ or N depending on whether the k-th user belongs to $\mathcal{S}_m$.

III. Proposed Smooth Characterization Scheme for AP Switching and Power Allocation

Under the constraints of limited AP transmit power and the requirement to achieve the desired MASR level in all regions, a JAPSPA optimization problem is formulated with the objective of maximizing the overall quality of service for all users. Specifically, the problem is mathematically formulated as

$$\mathcal{P}_1: \max_{\mathbf{a},\mathbf{\Theta}^c,\mathbf{\Theta}^s} \min_{k\in\mathcal{K}} \ \mathrm{SE}_k(\mathbf{\Theta}^c,\mathbf{\Theta}^s) \tag{12a}$$

$$\text{s.t.} \quad \mathrm{MASR}_l(\mathbf{\Theta}^c,\mathbf{\Theta}^s) \geq \kappa, \forall l \in \mathcal{L}, \tag{12b}$$

$$\sum_{k\in\mathcal{K}} \eta^c_{mk}\gamma_{mk}\nu_{mk} \leq a_m, \forall m \in \mathcal{M}, \tag{12c}$$

$$\sum_{l\in\mathcal{L}} \eta^s_{ml} \leq \frac{(1-a_m)}{N}, \forall m \in \mathcal{M}, \tag{12d}$$

$$a_m \in \{0,1\}, \forall m \in \mathcal{M}, \tag{12e}$$

where κ denotes the desired MASR level, while (12c) and (12d) represent the C-AP and S-AP transmit power constraints, respectively. The appearance of a_m on the right-hand side of these two constraints serves to enforce the mutual exclusivity of the communication and sensing power allocations. Specifically, if $a_m = 1$, the sensing power is forced to zero (i.e., $0 \leq \sum_{l\in\mathcal{L}} \eta^s_{ml} \leq \frac{(1-a_m)}{N} = 0$), and conversely.

Note that $\mathcal{P}_1$ is a highly intractable problem due to its mixture of continuous and discrete variables, the non-convex nature of both the objective function and (12b), and the coupling among the optimization variables. Although [1] applies continuous relaxation and SCA framework to solve it, that algorithm relies on interior point method with high computational complexity, which struggles to meet real-time requirements.

A. Establishment of An Approximated Continuous Problem

Although the coupling among variables increases the complexity of the optimization problem, it also provides a key insight for solving it [8]. This observation motivates us to leverage the information from the continuous variables to characterize the discrete ones, thereby approximating the original problem in a continuous domain. More precisely, the following smooth characterization function is introduced

$$\sigma\left(\mathbf{\Theta}^c_m\right) = \frac{\|\mathbf{\Theta}^c_m\|^2}{\|\mathbf{\Theta}^c_m\|^2 + \delta}, \quad \mathbf{\Theta}^c_m \in \mathbb{R}_+^{1\times K}, \tag{13}$$

where δ is a small positive constant to control the approximation degree. The function $\sigma\left(\mathbf{\Theta}^c_m\right)$ is motivated by the observed coupling between $\mathbf{\Theta}^c_m$ and a_m: when $\|\mathbf{\Theta}^c_m\| = 0$, the AP operates in sensing mode ($a_m = 0$), while for any $\|\mathbf{\Theta}^c_m\| > 0 \Longleftrightarrow a_m = 1$, forming a step-function mapping. However, this step function is non-smooth and unsuitable for algorithm design. Therefore, we propose $\sigma\left(\mathbf{\Theta}^c_m\right)$ as a smooth approximation to this mapping. For notational simplicity, we concatenate all optimization variables into a single matrix, denoted by $\mathbf{\Theta} \triangleq [\mathbf{\Theta}^c, \mathbf{\Theta}^s] \in \mathbb{R}_+^{M\times(K+L)}$. Based on this, $\mathcal{P}_1$ can be approximated and transformed into the following form

$$\mathcal{P}_2: \max_{\mathbf{\Theta}} f(\mathbf{\Theta}) \triangleq \min_{k\in\mathcal{K}} \ \mathrm{SINR}_k(\mathbf{\Theta}) \tag{14a}$$

$$\text{s.t.} \quad \mathrm{MASR}_l(\mathbf{\Theta}) \geq \kappa, \forall l \in \mathcal{L}, \tag{14b}$$

$$\sum_{k\in\mathcal{K}} \eta^c_{mk}\gamma_{mk}\nu_{mk} \leq 1, \forall m \in \mathcal{M}, \tag{14c}$$

$$N\sum_{l\in\mathcal{L}} \eta^s_{ml} \leq 1 - \frac{\|\mathbf{\Theta}^c_m\|^2}{\|\mathbf{\Theta}^c_m\|^2 + \delta}, \forall m \in \mathcal{M}. \tag{14d}$$

B. The Proposed SC-JAPSPA Algorithm

The transformation eliminates discrete constraints, but the resulting problem $\mathcal{P}_2$ is still hindered by non-smooth and non-convex elements. To tackle this challenge with low complexity, we adopt the penalty method as well as APG-AM algorithm.

Firstly, noting that the objective function $f(\mathbf{\Theta})$ is non-smooth, we employ the following log-sum-exp function for high-precision smooth approximation

$$\begin{aligned} f(\mathbf{\Theta}) &= \min_{k\in\mathcal{K}} \ \mathrm{SINR}_k\left(\mathbf{\Theta}\right) \approx -f_\chi(\mathbf{\Theta}) \\ &\triangleq -\frac{1}{\chi}\log\left(\frac{1}{K}\sum_{k\in\mathcal{K}} \exp\left(-\chi \mathrm{SINR}_k\left(\mathbf{\Theta}\right)\right)\right), \end{aligned} \tag{15}$$

where $\chi > 0$ is the smoothness parameter. The negative sign preceding function $f_\chi(\mathbf{\Theta})$ is introduced to transform the problem into a more easily described minimization formulation. It can be proved that $-f_\chi(\mathbf{\Theta})$ is a differentiable approximation of $f(\mathbf{\Theta})$ with a numerical accuracy of $\frac{\ln K}{\chi}$, i.e. $f(\mathbf{\Theta}) + \frac{\ln K}{\chi} \geq -f_\chi(\mathbf{\Theta}) \geq f(\mathbf{\Theta})$. Therefore, with a sufficiently large χ, $-f_\chi(\mathbf{\Theta})$ can serve as a high precision surrogate function for $f(\mathbf{\Theta})$.

Subsequently, to handle the non-convex constraints (14b) and (14d), we introduce the following quadratic loss function

$$Q_1(\mathbf{\Theta}) \triangleq \sum_{l\in\mathcal{L}} \left[\max\left(0, \kappa - \mathrm{MASR}_l\left(\mathbf{\Theta}\right)\right)\right]^2, \tag{16}$$

$$\mathrm{SINR}_k\left(\mathbf{\Theta}^c,\mathbf{\Theta}^s\right) = \frac{\rho_d\left(\sum_{m\in\mathcal{M}}\sqrt{\eta^c_{mk}}\gamma_{mk}\varrho_{mk}\right)^2}{1+\rho_d N\sum_{m\in\mathcal{M}}\sum_{l\in\mathcal{L}}\eta^s_{ml}\beta_{mk}+\rho_d\sum_{m\in\mathcal{M}}\sum_{k'\in\mathcal{K}}\left(\eta^c_{mk'}\gamma_{mk'}\varpi_{mk}\right)}, \tag{8}$$

$$\mathrm{MASR}_l\left(\mathbf{\Theta}^c,\mathbf{\Theta}^s\right) = \frac{\sum_{m\in\mathcal{M}} N^2\eta^s_{ml}}{\sum_{m\in\mathcal{M}}\sum_{k\in\mathcal{K}}\eta^c_{mk}\gamma_{mk}\nu_{mk}+\sum_{m\in\mathcal{M}}\sum_{l'\in\mathcal{L}\setminus l}\eta^s_{ml'}|\mathbf{a}_N^\dagger(\theta_{ml})\mathbf{a}_N(\theta_{ml'})|^2}. \tag{11}$$

$$Q_2(\boldsymbol{\Theta}) \triangleq \sum_{m\in\mathcal{M}} \left[\max\left(0, N\sum_{l\in\mathcal{L}}\eta_{ml}^s + \frac{\|\boldsymbol{\Theta}_m^c\|^2}{\|\boldsymbol{\Theta}_m^c\|^2+\delta} - 1\right)\right]^2. \tag{17}$$

Then, the penalized objective function can be expressed as

$$H_{\chi,\boldsymbol{\lambda}}(\boldsymbol{\Theta}) \triangleq f_\chi(\boldsymbol{\Theta}) + \sum_{i=1}^{2}\lambda_i\mu_i Q_i(\boldsymbol{\Theta}). \tag{18}$$

Here, λ_1 and λ_2 are penalty coefficients, while μ_1 and μ_2 denote the scaling coefficients designed to balance the magnitudes of the penalty terms and the main objective $f_\chi(\boldsymbol{\Theta})$, thereby facilitating stable convergence in the subsequent iterations.

For the convex constraint (14c), we adopt the following indicator function to facilitate subsequent proximal operations

$$I(\boldsymbol{\Theta}^c) \triangleq \begin{cases} 0, & \text{if } \boldsymbol{\Theta}^c \in \mathcal{C} \triangleq \{(14c), \boldsymbol{\Theta}^c \geq \mathbf{0}\}, \\ \infty, & \text{otherwise.} \end{cases} \tag{19}$$

Ultimately, $\mathcal{P}_2$ can be reformulated into the following unconstrained problem $\mathcal{P}_3$

$$\mathcal{P}_3: \quad \min_{\boldsymbol{\Theta}} \quad H_{\chi,\boldsymbol{\lambda}}(\boldsymbol{\Theta}) + I(\boldsymbol{\Theta}^c). \tag{20}$$

Now, $\mathcal{P}_3$ possesses a structure of a non-convex smooth function plus a non-smooth convex indicator, making it amenable to efficient solution via the APG-AM method [8]. Specifically, let t denote the current APG-AM iteration index. In addition to the optimization variable $\boldsymbol{\Theta}$ that we aim to obtain, the APG-AM algorithm also introduces the auxiliary variables $\mathbf{Z} \in \mathbb{R}_+^{M\times(K+L)}$, and updates the optimization variables according to the following criterion

$$\boldsymbol{\Theta}^{(t)} = \text{prox}_{\alpha^{(t)},I}\left(\mathbf{Z}^{(t)} - \alpha^{(t)}\nabla H_{\chi,\boldsymbol{\lambda}}(\mathbf{Z}^{(t)})\right), \tag{21}$$

where $\alpha^{(t)}$ represents the step size at the t-th iteration and $\text{prox}_{\alpha^{(t)},I}$ is the so-called proximal operator defined as [8][1]

$$\text{prox}_{\alpha^{(t)},I}(\mathbf{x}) = \underset{\boldsymbol{\Theta}\in\mathbb{R}_+^{M\times K}}{\arg\min}\left(I(\boldsymbol{\Theta}) + \frac{1}{2\alpha^{(t)}}\|\boldsymbol{\Theta}-\mathbf{X}\|^2\right). \tag{22}$$

In particular, utilizing the defined indicator function $I(\boldsymbol{\Theta}^c)$, the proximal operator can be simplified into the following projection operation

$$\text{prox}_{\mathcal{C}}(\mathbf{X}) = \underset{\boldsymbol{\Theta}\in\mathcal{C}}{\arg\min}\ \|\boldsymbol{\Theta}-\mathbf{X}\|^2, \tag{23}$$

which is a standard convex optimization problem. Since the convex set $\mathcal{C}$ is independent of the PAC for S-APs, the aforementioned projection operation will only adjust the communication PAC. Specifically, let $\tilde{\mathbf{X}} \in \mathbb{R}^{M\times K}$ denote the matrix constituted by the first K columns of $\mathbf{X}$, such that $\text{prox}_{\mathcal{C}}(\mathbf{X}) = \text{prox}_{\mathcal{C}}(\tilde{\mathbf{X}}) = \underset{\boldsymbol{\Theta}^c\in\mathcal{C}}{\arg\min}\ \|\boldsymbol{\Theta}^c - \tilde{\mathbf{X}}\|^2$. We can now obtain the following result.

[1]Strictly speaking, the norm in this proximal operator should be the matrix Frobenius norm. For simplicity, this paper does not distinguish between the Frobenius norm and the ℓ_2-norm, as the former can be equivalently transformed into the latter by vectorizing the matrix.

Lemma 1. *For given $\tilde{\mathbf{X}}$, the projection $\text{prox}_{\mathcal{C}}(\tilde{\mathbf{X}})$ for the communication PAC is given by the following analytical solution*

$$\eta_{mk}^{c,\star} = \max\left(0,\ \tilde{x}_{mk} - \tfrac{\xi_m}{2}\gamma_{mk}\nu_{mk}\right). \tag{24}$$

Here, $\tilde{x}_{mk}$ is the (m,k)-th entry of $\tilde{\mathbf{X}}$ and ξ_m is the Lagrange multiplier determined according to the following condition

$$\xi_m = \begin{cases} 0, \ \textit{if } \sum_{k\in\mathcal{K}}\max(0,\tilde{x}_{mk})\gamma_{mk}\nu_{mk} \leq 1, \\ \text{the root of (29)}, \ \text{otherwise.} \end{cases} \tag{25}$$

Proof: First, since the power constraints in the convex set $\mathcal{C}$ are imposed individually on each AP, and the proximal objective in (23) is separable, the original problem in (23) can be decomposed into the following M independent subproblems:

$$\mathcal{P}_4: \min_{\boldsymbol{\Theta}_m^c\in\mathbb{R}_+^{1\times K}} \sum_{k\in\mathcal{K}}\left(\eta_{mk}^c - \tilde{x}_{mk}\right)^2 \tag{26a}$$

$$\text{s.t.} \sum_{k\in\mathcal{K}}\eta_{mk}^c\gamma_{mk}\nu_{mk} \leq 1. \tag{26b}$$

Subsequently, we can formulate the *Lagrangian* function $\mathcal{L}(\boldsymbol{\Theta}_m^c, \xi_m, \boldsymbol{\zeta})$ by introducing non-negative *Lagrangian* multiplier ξ_m and $\boldsymbol{\zeta} \in \mathbb{R}^K$ as

$$\begin{aligned}\mathcal{L}(\boldsymbol{\Theta}_m^c, \xi_m, \boldsymbol{\zeta}) \triangleq &\sum_{k\in\mathcal{K}}\left(\eta_{mk}^c - \tilde{x}_{mk}\right)^2 - \sum_{k\in\mathcal{K}}\zeta_k\eta_{mk}^c \\ &+ \xi_m\left(\sum_{k\in\mathcal{K}}\eta_{mk}^c\gamma_{mk}\nu_{mk} - 1\right).\end{aligned} \tag{27}$$

To obtain the optimal PAC for C-APs, we apply the *Karush-Kuhn-Tucker* (KKT) conditions and derive the corresponding stationarity and complementary slackness conditions of the dual problem as

$$2(\eta_{mk}^c - \tilde{x}_{mk}) - \zeta_k + \xi_m\,\gamma_{mk}\,\nu_{mk} = 0, \forall k \in \mathcal{K}, \tag{28a}$$

$$\xi_m\left(\sum_{k\in\mathcal{K}}\eta_{mk}^c\gamma_{mk}\nu_{mk} - 1\right) = 0,\ \zeta_k\eta_{mk}^c = 0, \forall k \in \mathcal{K}. \tag{28b}$$

By combining the above two conditions, the following unified optimal closed-form solution can be easily obtained

$$\eta_{mk}^{c,\star} = \max\left(0,\ \tilde{x}_{mk} - \tfrac{\xi_m}{2}\gamma_{mk}\nu_{mk}\right).$$

Here, ξ_m is the Lagrange multiplier to be determined, whose value is obtained via the complementary slackness condition. Specifically, if $\sum_{k\in\mathcal{K}}\max(0,\tilde{x}_{mk})\gamma_{mk}\nu_{mk} \leq 1$, then $\xi_m = 0$ and the optimal solution is $\eta_{mk}^{c,\star} = \max(0,\tilde{x}_{mk})$. Otherwise, $\xi_m > 0$ is the unique root of the following scalar equation

$$\sum\nolimits_{k\in\mathcal{K}}\max\left(0,\ \tilde{x}_{mk} - \tfrac{\xi_m}{2}\gamma_{mk}\nu_{mk}\right)\gamma_{mk}\nu_{mk} = 1, \tag{29}$$

which is continuous and strictly decreasing in ξ_m. This solution essentially corresponds to a soft-thresholding operation, where the value of ξ_m can be efficiently obtained using bisection search or fixed-point iteration. The resulting computation has a $\mathcal{O}(K)$ complexity order, ensuring the low-complexity implementation of the proposed algorithm. ■

Algorithm 1: The **SC-JAPSPA** algorithm for $\mathcal{P}_3$

Input : $\mathbf{Z}^{(1)} = \mathbf{\Theta}^{(0)}, \mu_1 = 10^3, \mu_2 = 10, \beta = 2, \omega = 0.5, \boldsymbol{\lambda} = \mathbf{1}, t = 1, \varepsilon = 10^{-3}, \alpha^{(t)} = 10^{-3}$

repeat // Penalty loop
  repeat // APG-AM loop
    update $\mathbf{\Theta}^{(t)}$ via (21) and $\mathbf{v}^{(t)}$ via (30)
    update $\mathbf{Z}^{(t+1)}$ and β via (31)
    if $|H_{\chi,\boldsymbol{\lambda}}(\mathbf{\Theta}^{(t)}) - H_{\chi,\boldsymbol{\lambda}}(\mathbf{\Theta}^{(t-1)})| > \varepsilon$ **then**
      $t = t + 1$
    end
  until $|H_{\chi,\boldsymbol{\lambda}}(\mathbf{\Theta}^{(t)}) - H_{\chi,\boldsymbol{\lambda}}(\mathbf{\Theta}^{(t-1)})| \leq \varepsilon$;
  increase the penalty coefficients $\lambda_i = 10\lambda_i, i = 1, 2$
until $|Q_1(\mathbf{\Theta}^{(t)}) - Q_1(\mathbf{\Theta}^{(t-1)})| \leq \varepsilon$ as well as $|Q_2(\mathbf{\Theta}^{(t)}) - Q_2(\mathbf{\Theta}^{(t-1)})| \leq \varepsilon$;

Output: Stationary power allocation coefficients: $\mathbf{\Theta}^{\star}$

In a nutshell, given fixed $\boldsymbol{\lambda}$, the APG-AM algorithm is employed to efficiently solve the optimization problem involving a non-smooth indicator function. When the penalty function exceeds a given tolerance, the penalty coefficients will be increased and then the problem $\mathcal{P}_3$ is re-solved. To summarize, the proposed **SC-JAPSPA** algorithm for solving the approximated continuous problem $\mathcal{P}_3$ is outlined in **Algorithm 1**.

To further accelerate the convergence, APG-AM adjusts the optimization variables as follows

$$\mathbf{V}^{(t)} = \mathbf{\Theta}^{(t)} + \beta \left(\mathbf{\Theta}^{(t)} - \mathbf{\Theta}^{(t-1)} \right), \tag{30}$$

with

$$\begin{cases} \text{If } H_{\chi,\boldsymbol{\lambda}}(\mathbf{\Theta}^{(t)}) \leq H_{\chi,\boldsymbol{\lambda}}(\mathbf{V}^{(t)}) \\ \qquad \mathbf{Z}^{(t+1)} = \mathbf{\Theta}^{(t)}, \beta = \omega \cdot \beta, \\ \text{If } H_{\chi,\boldsymbol{\lambda}}(\mathbf{\Theta}^{(t)}) > H_{\chi,\boldsymbol{\lambda}}(\mathbf{V}^{(t)}) \\ \qquad \mathbf{Z}^{(t+1)} = \mathbf{v}^{(t)}, \beta = \min\{\frac{\beta}{\omega}, 1\}. \end{cases} \tag{31}$$

Here, β denotes the momentum parameter and $\omega \in (0, 1)$ is the scaling factor. Moreover, $\mathbf{V} \in \mathbb{R}^{M \times (K+L)}$ is an extrapolated variable. When its corresponding function value is smaller, i.e. $H_{\chi,\boldsymbol{\lambda}}(\mathbf{\Theta}^{(t)}) > H_{\chi,\boldsymbol{\lambda}}(\mathbf{V}^{(t)})$, the momentum is increased to further exploit the opportunity for accelerating.

C. Complexity and Convergence Analysis

Since the proximal in (21) requires the gradient descent point of the smooth term, it is necessary to compute $\nabla H_{\chi,\boldsymbol{\lambda}}(\cdot)$ and prove its *Lipschitz* smoothness, which serves as the core condition for the convergence of the APG-AM algorithm [8]. Therefore, we present the following proposition.

Proposition 1. *The closed-form expression of $\nabla H_{\chi,\boldsymbol{\lambda}}(\cdot)$ can be efficiently obtained by the gradient rule for multi-variable function, which has $\mathcal{O}(M \max(K, L)^2)$ computational complexity order. Furthermore, $H_{\chi,\boldsymbol{\lambda}}(\cdot)$ achieves the L_H Lipschitz smoothness property, i.e. there exists a constant $L_H > 0$, such that the following inequality holds*

$$\|\nabla H_{\chi,\boldsymbol{\lambda}}(\mathbf{\Theta}) - \nabla H_{\chi,\boldsymbol{\lambda}}(\mathbf{Z})\| \leq L_H \|\mathbf{\Theta} - \mathbf{Z}\|, \ \forall \mathbf{\Theta}, \mathbf{Z} \in \mathcal{C}. \tag{32}$$

The computation of $\nabla H_{\chi,\boldsymbol{\lambda}}(\cdot)$ and the proof of its *Lipschitz* smoothness are analogous to those presented in Appendices B and C of [8], respectively, and are omitted here for brevity. Clearly, the computational complexity of **Algorithm 1** is dominated by the gradient computation, resulting in an overall complexity of $\mathcal{O}(I_P I_A M \max(K, L)^2)$ for the **SC-JAPSPA** algorithm, where I_P and I_A denote the numbers of penalty and APG-AM iterations, respectively. Building upon Proposition 1, we proceed to analyze the convergence of the proposed algorithm, which comprises a two-layer iterative process. First, regarding the outer penalty loop, the feasibility of $\mathcal{P}_2$ guarantees that the penalty term vanishes as the penalty coefficient $\boldsymbol{\lambda}$ increases. Furthermore, $\mathcal{P}_2$ and $\mathcal{P}_3$ satisfy strong duality, i.e., $\min\limits_{\mathbf{\Theta} \in \mathcal{H}} -f(\mathbf{\Theta}) = \sup\limits_{\boldsymbol{\lambda} \geq \mathbf{0}} \min\limits_{\mathbf{\Theta} \in \mathcal{C}} H_{\chi,\boldsymbol{\lambda}}(\mathbf{\Theta})$, where $\mathcal{H} \triangleq \{(14b), (14c), (14d)\}$. Subsequently, for the inner APG-AM loop, provided the step size $\alpha^{(t)}$ is smaller than $1/L_H$, the algorithm aligns with the majorization-minimization (MM) framework. By iteratively optimizing a surrogate upper bound of the original objective function, the inner loop converges to a stationary point of $\mathcal{P}_3$. Consequently, the overall convergence of the **SC-JAPSPA** algorithm is established.

IV. Numerical Results

In this section, we evaluate the performance of the proposed **SC-JAPSPA** algorithm in terms of SE. The channel and sensing parameters are configured identically to those in [1]. By default, we set $M = 20, K = 8, N = 16, L = 4$ and $\kappa = 6$ dB. The parameter configurations for the proposed algorithm are summarized in **Algorithm 1**. Moreover, the initial PAC $\boldsymbol{\theta}^{(0)}$ can be obtained via uniform power allocation. Specifically, the benchmark algorithms considered for comparison are as follows: (1) **SCA-JAPSPA** [1]: Using the SCA framework to solve the joint optimization problem, which incurs $\mathcal{O}\left(M^{3.5} \max(K, L)^{3.5}\right)$ computation complexity order per iteration. (2) Greeedy (**G-JAPSPA**) [1]: A greedy algorithm is first employed for AP mode selection, after which power allocation is performed under the fixed mode configuration.

Figure 2 compares the cumulative distribution function (CDF) of the SE for the proposed algorithm and benchmark methods under varying system scales. Specifically, when $M = 60$, the 5%-outage rates are 4.83 bit/s/Hz and 4.67 bit/s/Hz for **SCA-JAPSPA** and **SC-JAPSPA**, respectively. With a smaller number of APs (i.e. $M = 10$), the system may be unable to fully satisfy the sensing requirements, causing some users to experience zero rate. In comparison with **G-JAPSPA**, the proposed algorithm effectively reduces the number of users that cannot maintain reliable communication. The results indicate that **SC-JAPSPA** consistently almost matches the performance of **SCA-JAPSPA**, ensuring reliable communication for all users to the greatest extent possible under the constraint of sensing requirements. In addition, Table I presents the actual runtime of several algorithms under different system scales. It is evident that, compared with the two benchmark methods, the proposed algorithm significantly reduces the runtime while achieving comparable communication performance. These results demonstrate the effectiveness of the proposed algorithm, highlighting its suitability as a

TABLE I
COMPARISON BETWEEN THE EXECUTION TIME (IN SECONDS)

Algorithm	Number of APs (M)				Number of Users (K)				Number of Sensing Zones (L)			
	20	30	40	60	4	8	12	20	2	4	8	12
SCA-JAPSPA [1]	173.61	269.93	375.27	424.84	152.64	173.61	213.43	284.31	143.59	173.61	202.86	243.03
G-JAPSPA [1]	25.88	31.15	35.21	58.23	17.95	25.88	33.43	45.34	15.28	25.88	31.07	37.29
SC-JAPSPA (this work)	8.57	14.68	19.34	25.93	4.13	8.57	13.85	17.34	3.02	8.57	11.39	14.51

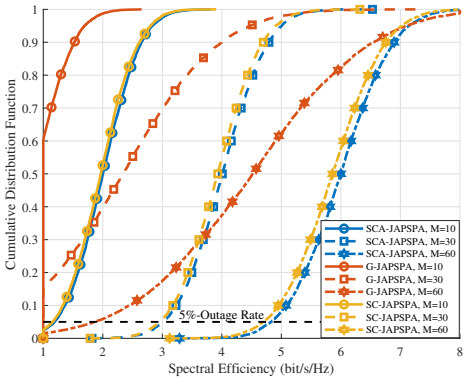

Fig. 2. CDF of the per user SE for different algorithms.

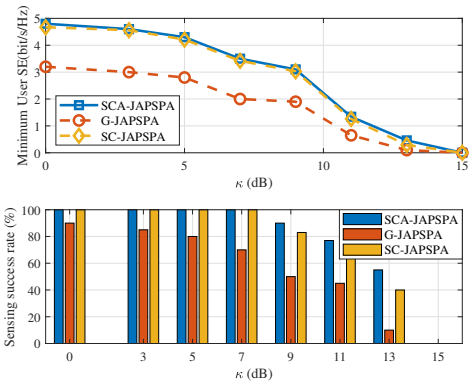

Fig. 3. Minimum user SE and sensing rate versus κ.

joint sensing and communication solution for scenarios with stringent real-time requirements.

Figure 3 depicts the impact of the sensing threshold κ on both the average minimum user SE and the sensing success probability. In general, stringent sensing constraints (i.e., higher κ) inevitably impair the sensing success rates across all evaluated methods. Within the moderate regime of κ, **G-JAPSPA** suffers from a precipitous decline in SE. In contrast, **SCA-JAPSPA** and **SC-JAPSPA** demonstrate superior robustness with a much milder decay. However, once κ surpasses 11 dB, the optimization problems for **SCA-JAPSPA** and **SC-JAPSPA** frequently become infeasible. This results in a sudden performance collapse, where infeasible instances are recorded as zero throughput whereas sensing fails in the statistical average sense.

V. CONCLUSION

This paper addressed the joint AP-mode switching and PAC problem in CF-mMIMO ISAC networks. By exploiting the continuous–discrete coupling between AP states and transmit coefficients, we derived a smooth continuous surrogate that bypasses binary variables while preserving exclusivity. The resulting non-convex program is solved with the **SC-JAPSPA** algorithm, which integrates penalty reformulation and accelerated proximal gradient with adaptive momentum. Computational time is reduced by an order of magnitude to $\mathcal{O}(I_P I_A M \max(K, L)^2)$, while our simulations showed that 95% of the optimal max–min SE is retained with guaranteed MASR sensing. To sum up, the proposed **SC-JAPSPA** offers a scalable, real-time solution for large-scale ISAC deployments.

ACKNOWLEDGMENT

This work was supported in part by the National Science and Technology Major Projects of China under Grant 2025ZD1301800, SEU Innovation Capability Enhancement Plan for Doctoral Students CXJH_SEU 26105, and in part by the European Research Council (ERC) under the European Union's Horizon 2020 research and innovation programme (grant agreement No. 101001331).

REFERENCES

[1] M. Elfiatoure, M. Mohammadi, H. Q. Ngo, H. Shin, and M. Matthaiou, "Multiple-target detection in cell-free massive MIMO-assisted ISAC," *IEEE Trans. Wireless Commun.*, vol. 24, no. 5, pp. 4283-4298, May 2025.

[2] Z. Behdad *et al.*, "Multi-static target detection and power allocation for integrated sensing and communication in cell-free massive MIMO," *IEEE Trans. Wireless Commun.*, vol. 23, no. 9, pp. 11580-11596, Sept. 2024.

[3] U. Demirhan and A. Alkhateeb, "Cell-free ISAC MIMO systems: Joint sensing and communication beamforming," *IEEE Trans. Commun.*, vol. 73, no. 6, pp. 4454-4468, Jun. 2025.

[4] H. Q. Ngo, G. Interdonato, E. G. Larsson, G. Caire, and J. G. Andrews, "Ultradense cell-free massive MIMO for 6G: Technical overview and open questions," *Proc. IEEE*, vol. 112, no. 7, pp. 805-831, July 2024.

[5] Z. Wang, L. Liang, S. Lyu, Y. Xia, Y. Huang, and D. W. K. Ng, "Efficient statistical linear precoding for downlink massive MIMO systems," *IEEE Trans. Wireless Commun.*, vol. 23, no. 10, pp. 14805-14818, Oct. 2024.

[6] Y. Gao *et al.*, "Artificial intelligence enabled joint channel estimation and signal detection for massive MIMO systems," *Chin. J. Electron.*, vol. 35, no. 1, pp. 178–195, Jan. 2026.

[7] M. Mohammadi *et al.*, "Network-assisted full-duplex cell-free massive MIMO: Spectral and energy efficiencies," *IEEE J. Sel. Areas Commun.*, vol. 41, no. 9, pp. 2833–2851, Sept. 2023.

[8] B. Yan *et al.*, "Efficient energy efficiency optimization method for cell-free massive MIMO-enabled URLLC downlink systems," *IEEE Trans. Wireless Commun.*, vol. 25, pp. 4851-4868, 2026.

[9] G. Interdonato, M. Karlsson, E. Björnson, and E. G. Larsson, "Local partial zero-forcing precoding for cell-free massive MIMO," *IEEE Trans. Wireless Commun.*, vol. 19, no. 7, pp. 4758-4774, Jul. 2020.